ELSEVIER

Journal of Alloys and Compounds 253–254 (1997) 445–448

Journal of ALLOYS AND COMPOUNDS

Hydrogen hopping rates and the order–disorder transitions in sub-stoichiometric lanthanum trihydride

R.G. Barnes[a,*], B.J. Beaudry[a], D.R. Torgeson[a], C.T. Chang[b], R.B. Creel[c]

[a]*Ames Laboratory, USDOE, and Department of Physics, Iowa State University, Ames, IA 50011, USA*
[b]*MR Imaging Laboratory, Texas A and M University, College Station, TX 77843, USA*
[c]*Department of Physics, University of Akron, Akron, OH 44325, USA*

Abstract

Extensive measurements of proton magnetic resonance lineshapes and spin–lattice relaxation rates in sub-stoichiometric lanthanum trihydrides, prepared from highest purity La metal, furnish clear evidence for the coexistence of ordered and disordered hydrogen sublattices over an extended temperature range terminating with the onset of semiconducting behavior. This phenomenon persists even at the stoichiometric limit, LaH_3. Analysis of resonance lineshape intensities yields $H_t=0.080\pm0.020$ eV for the enthalpy of the order–disorder transition in $LaH_{2.99}$, and analysis of intensities in relaxation rate measurements yields $H_t=0.066\pm0.020$ eV for this enthalpy in $LaH_{2.90}$. A second, higher temperature transition in the hydrogen hopping rate appears to coincide with the onset of semiconducting behavior.

Keywords: Lanthanum trihydride; Order–disorder transition; Nuclear magnetic resonance

1. Introduction

In common with the trihydrides of the other light rare-earth metals (i.e., Ce, Pr, Nd), lanthanum trihydrides exhibit two co-existing proton (^1H) magnetic resonances in certain ranges of composition and temperature [1–3]. An example of this behavior is shown in Fig. 1 for $LaH_{2.93}$. Typically, with decreasing temperature, the narrow resonance observed at 300 K and above changes gradually into a broad resonance superimposed on the narrow one. Both resonances coexist over some further decreasing temperature range, after which the narrow line also broadens and decreases in intensity so that the two resonances become indistinguishable. It is also evident from the figure that the two resonances are unshifted with respect to one another (however, this is not true for CeH_x etc. [3]). This fact is also very evident in the pulse measurements of the ^1H spin–lattice relaxation rate, R_1, in that the entire two-component free-induction decay signal can be brought into resonance simultaneously. An example of an inversion–recovery sequence measurement of R_1 is shown in Fig. 2 for $LaH_{2.80}$ at 233 K. The narrow resonance recovers more quickly, showing that it has the greater R_1. For $x\leq2.50$ only a single ^1H resonance is observed; for $2.5\leq x\leq2.85$ the region of two resonances agrees reasonably with the LaH_2–LaH_3 phase diagram [4]; but for $2.85\leq x\leq3.00$ where the phase diagram indicates single-phase behavior,

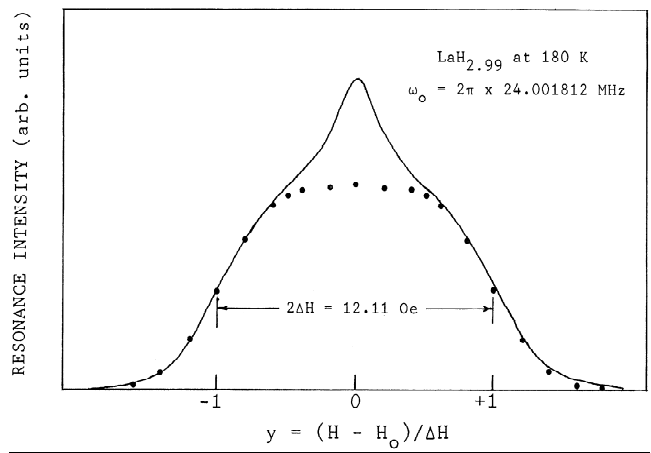

Fig. 1. Proton magnetic resonance lineshape in $LaH_{2.99}$ at 180 K at a resonance frequency of 24 MHz. The solid points show the fit of the function, $g(y)=a\cdot\exp(-b\cdot|y|^n)$, with $n=3.6$, to the broad-line component (see text).

*Corresponding author.

PII S0925-8388(96)02969-6

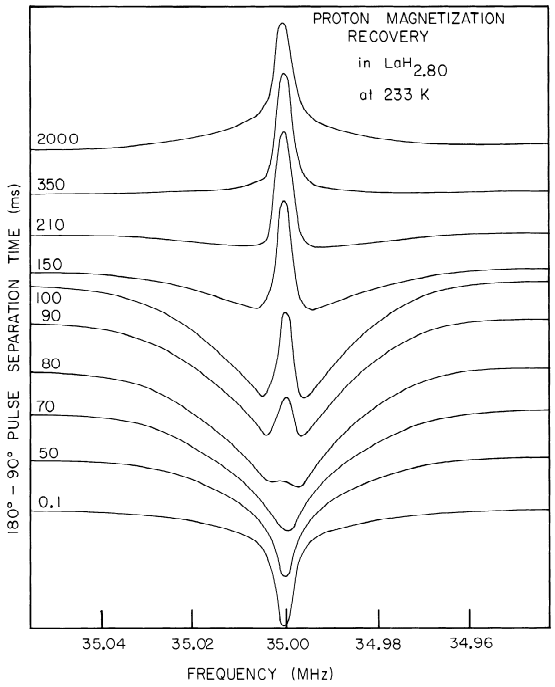

Fig. 2. Sequence of resonance intensity signals (Fourier transforms of free-induction decay signals) in $LaH_{2.80}$ at 233 K at a resonance frequency of 35.00 MHz. The individual traces are identified by the 180°–90° pulse separation time (in milliseconds) along the abscissa. The narrow component of the composite resonance recovers much more quickly than the broad component.

^{1}H NMR continues to reveal multi-phase characteristics. In this brief report, we concentrate on this latter range of composition.

The composition range $x \geq 2.85$ is also that in which LaH_x undergoes a metal–semiconductor transition with increasing temperature most sharply defined at $x \approx 2.90$ [5]. It is now generally accepted that this transition occurs when a delocalized band of states at the Fermi energy, E_F, associated with the low-temperature superlattice of octahedral-site hydrogen vacancies, becomes localized and its mobility is quenched when the super-lattice collapses with increasing temperature at $T \approx 260$ K [6]. For $2.50 \leq x \leq 2.85$, X-ray diffraction shows the O-site ordering to be capable of causing a tetragonal distortion of the La lattice, whereas for $x \geq 2.85$ no distortion is evident [4,7]. However, neutron diffraction at $x=3$ has shown the presence of superlattice lines (not indexed) whose intensity decreases smoothly to zero with increasing temperature at $T \approx 240$ K [8]. Heat capacity measurements of $LaH_{3.0}$ showed two broad peaks at 241 K and 270 K [9]. The present NMR study supports the occurrence of two successive order–disorder transitions.

2. Experimental aspects

The samples investigated in this work are those used in an investigation of the electronic density-of-states (DOS) in this system [10]. They were prepared from the highest-purity Ames Lab lanthanum available (batch No. La-4783), having total magnetic rare-earth impurity content, determined by mass spectrometry, below 4.5 parts-per-million (ppm), and gadolinium content which is most significant for this work, less than 0.2 ppm. The magnetic resonance instrumentation has been described previously [11].

3. Results and discussion

The temperature dependence of the relative intensity of the narrow resonance in Fig. 1 yields an estimate of the enthalpy of the first, i.e., lower temperature, order–disorder transition. As shown in the figure, the broad component of the composite resonance is closely fitted with the lineshape function, $g(y)=a\cdot\exp(-b\cdot|y|^n)$ [12], where $y=(H-H_o/\Delta H)$, H and H_o being the magnetic field and field at resonance, respectively, and ΔH the half-width at the points of maximum slope determined from the lineshape derivative. Subtracting the resulting broad-line intensity I_B from the total intensity I_T yields the narrow resonance intensity I_N, and the ratio I_N/I_T its relative intensity. Fig. 3 shows the resulting plot of $\log(I_N/I_T)$ vs. $10^3/T$ from which, assuming that $I_N/I_T \sim \exp(-H_t/k_B T)$, we find $H_t = 0.080 \pm 0.020$ eV for the enthalpy of this order–disorder transition at $x=2.99$.

The total (measured) ^{1}H spin–lattice relaxation rate R_1 in LaH_x results from the sum of three contributions:

$$R_1 = R_{1e} + R_{1d} + R_{1p}, \quad (1)$$

where R_{1e} is the conduction electron contribution, R_{1d} the nuclear dipolar contribution, and R_{1p} that due to paramagnetic ion impurities. In metallic hydrides, $R_{1e}=C_e T$, where C_e depends on the DOS at the Fermi level, $N(E_F)$.

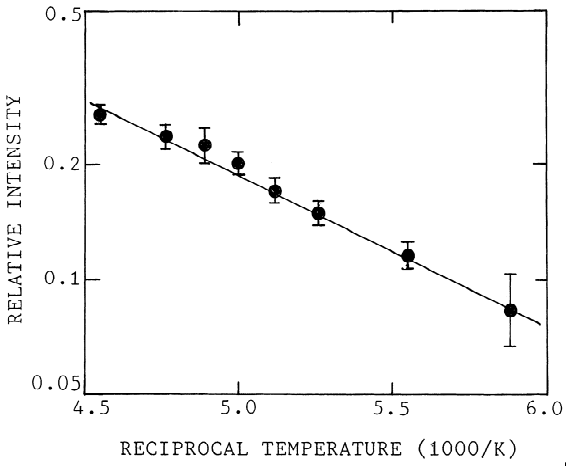

Fig. 3. Relative intensity of the narrow-line component of the proton resonance in $LaH_{2.99}$ measured at 24 MHz. The slope of the least-squares fit straight line yields an activation enthalpy, $H_t = 0.080 \pm 0.020$ eV for the order–disorder transition.

For $x \geq 2.85$ and the temperature range investigated, R_{1e} is essentially negligible. R_{1d} results from the fluctuating dipolar field accompanying hydrogen motion (diffusion) and reflects the temperature dependence of the hydrogen jump frequency, τ_d^{-1}, where τ_d is the mean dwell time. The rate R_{1p} depends on the impurity ion concentration and ion spin–lattice relaxation time, τ_i which is itself dependent on $N(E_F)$ in the metallic state and on phonon-driven interactions in the nonmetallic state.

At high x-values in LaH_x both tetrahedral (T) and octahedral (O) interstitial sites are fully, or nearly fully, occupied, so that T–T, T–O, O–T, and O–O diffusive jumps presumably occur. Despite this complexity, the R_{1d} data are very well represented by the usual simple Lorentzian spectral density formulation [13] employing a single correlation time equal to $\tau_d/2$:

$$R_{1d} = \frac{2\gamma_I^2 M_2}{3\omega_o}\left[\frac{y}{1+y^2} + \frac{4y}{1+4y^2}\right] \quad (2)$$

in which γ_I is the ^1H magnetogyric ratio, ω_o the resonance frequency, M_2 the resonance second moment in field units, and $y = \omega_o\tau_d/2$. M_2 is dominated by the ^1H–^1H contribution, but the ^1H–^{139}La contribution can be recognized phenomenologically by including it in M_2 (see inset in Fig. 4).

Relaxation rate data for $x = 2.90$ measured at 40 MHz are shown in Fig. 4. The data obviously divide into three regions: (1) a low-temperature region in which only one signal appears, (2) an intermediate range in which two signals coexist, and (3) a high-temperature region in which there is again only one resonance. An abrupt change in log R_1 vs. $10^3/T$ occurs at the transition from the intermediate to the high-temperature region, however no discontinuity in R_1 appears. Several features of these data are most significant: (1) In the region of two resonances, that with the slower rate, R_{1s}, dominates at low temperatures and is effectively extinguished at the transition, $T = 275 \pm 5$ K, being just 20% of the total intensity at 270 K. R_{1s} is the only relaxation rate found at low temperatures. The fast-relaxing component, R_{1f}, is first distinguishable at ~185 K (20% of total intensity) and continues to high temperatures where it becomes the only signal. (2) In the region of two resonances, the rates R_{1s} and R_{1f} display a remarkable parallelism, with $R_{1f} \approx 2.5 \cdot R_{1s}$. The activation enthalpies, based on linear fits to the slopes, are equal within experimental uncertainty, $H_a^{(low)} = 0.20 \pm 0.02$ eV. (3) Above 275 K the relaxation rate of the single resonance shows a substantially weaker enthalpy, $H_a^{(hi)} = 0.14 \pm 0.01$ eV. The solid curve in Fig. 4 shows Eq. (2) fit to the high-temperature points with a maximum rate, $R_{1f,max} = 40$ 5 s at $T_{max} = 248$ K. The inset in Fig. 4 shows the dependence on composition of $R_{1f,max}$. The solid curves are obtained from Eq. (2) using calculated M_2 values for the ^1H–^1H interaction only (lower curve) and including the ^1H–^{139}La contribution as well (upper curve). The experimental points fall roughly midway between the two estimates, and at high x-values $R_{1f,max}$ in the nominally pure samples is roughly 2.5 times greater than that in those of highest purity, showing the extreme importance of the R_{1p} contribution to R_1 in the semiconducting phase. The points for $x = 2.90$ and 3.00 high-purity samples fall below the lower curve because T_{max} for these x-values occurs at a temperature below the metal–semiconducting transition. Hence, $R_{1f,max} = 40.5\ s^{-1}$ is estimated by extrapolating the experimental values for $x < 2.90$.

From the data and analysis of Fig. 4 we draw the following conclusions: (1) Ordered and disordered phases already coexist for $T \approx 185$ K, perhaps as microdomains. (2) The apparent difference in hydrogen hopping rates, τ_d^{-1}, by a factor of ≈ 2.5, we attribute to a difference in site-blocking factors, since H_a is the same for both. (3) The fast-relaxing, disordered phase intensity increases steadily as $T \rightarrow 275$ K. Its temperature dependence yields $H_t = 0.066 \pm 0.020$ eV for the order–disorder transition enthalpy at $x = 2.90$, in good agreement with the result of Fig. 3 for $x = 2.99$. (4) The onset of semiconducting (variable-range hopping) behavior at $T \approx 275$ K is accompanied by a further increase in the hopping rate and a reduction in H_a in comparison to the disordered phase for $T \approx 275$ K.

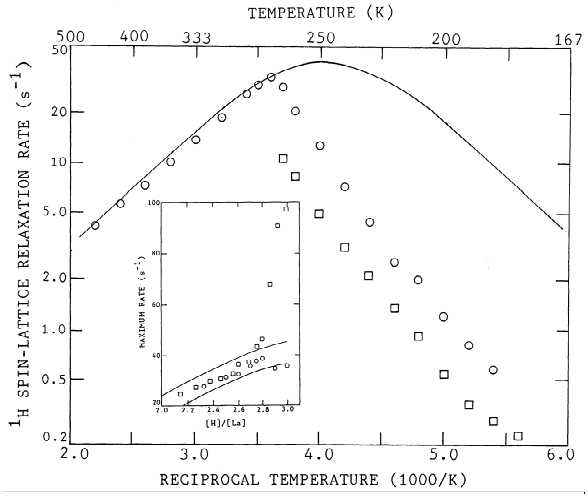

Fig. 4. Proton spin–lattice relaxation rates in $LaH_{2.90}$ measured at 40 MHz, showing the fast (circles) and slow (squares) relaxing components. The solid curve is the fit of Eq. (2) to the high-temperature data with $R_{1f,max} = 40.5\ s^{-1}$. The inset shows the x-dependence of $R_{1f,max}$ in LaH_x at 40 MHz for nominally high-purity samples (squares) and highest-purity (circles). The solid curves are described in text.

4. Summary and conclusions

The ^1H magnetic resonance lineshape and relaxation rate measurements reported here show clearly the occurrence of two transitions at which the hydrogen hopping rate in substoichiometric LaH_3 increases with increasing temperature. The first, lower-temperature transition extends from ≈185 to 275 K, the rate in the fast-diffusing,

disordered phase being ≈2.5–3.0 times greater than that in the slow-diffusing, ordered phase throughout this temperature range. We attribute this difference to a change in site-blocking accompanying the disordering. Based on lineshape intensities, the enthalpy of this transition is $H_t = 0.080 \pm 0.020$ eV at $x = 2.99$, and on the basis of relaxation rate measurements is $H_t = 0.066 \pm 0.020$ eV at $x = 2.90$. The higher-temperature transition is evident as a sharp decrease in activation enthalpy for hydrogen diffusion to $H_a = 0.14 \pm 0.01$ eV at 275 K, and we attribute this transition to the completion of the ordering process. Neutron diffraction has shown the O-site D atoms in LaD_3 to be displaced away from the site-centers along the eight ⟨111⟩ directions [14]. The present results are best understood as resulting from successive stages progressing from an ordered arrangement of the off-center atoms at low temperatures to random occupancy of those sites at intermediate temperatures, culminating in occupancy of the O-site-centers at temperatures above the metal–semiconductor transition temperature [9].

Acknowledgments

Dr. T.T. Phua contributed to some of the preliminary measurements. Ames Laboratory is operated for the U.S. Department of Energy by Iowa State University under Contract No. W-7405-Eng-82. This work was supported by the Director for Energy Research, Office of Basic Energy Sciences.

References

[1] D.S. Schreiber and R.M. Cotts, *Phys. Rev., 131* (1963) 1118.
[2] R. Göring, B. Schnabel and 0.J. Zogal, *Phys. Stat. Sol. (a), 59* (1980) K147.
[3] D. Zamir, R.G. Barnes, N. Salibi, R.M. Cotts, T.T. Phua, D.R. Torgeson and D.T. Peterson, *Phys. Rev. B, 29* (1984) 61.
[4] E. Boroch, K. Conder, Cai Ru-Xiu and E. Kaldis, *J. Less-Comm. Metals, 156* (1989) 259.
[5] J. Shinar, B. Dehner, R.G. Barnes and B.J. Beaudry, *Phys. Rev. Lett., 64* (1990) 563.
[6] P. Vajda, Hydrogen in Rare-Earth Metals, Including RH_{2+x} Phases, in K.A. Gschneidner Jr. and L. Eyring (eds.), *Handbook on the Physics and Chemistry of the Rare Earths*, Vol. 20, Elsevier, 1995, p. 251.
[7] P. Klavins, R.N. Shelton, R.G. Barnes and and B.J. Beaudry, *Phys. Rev. B, 29* (1984) 5349.
[8] J.J. Didesheim, K. Yvon, P. Fischer, W. Hälg and L. Schlapbach, *Phys. Lett., 78A* (1980) 111.
[9] T. Ito, B.J. Beaudry, K.A. Gschneidner Jr. and T. Takeshita, *Phys. Rev., 27* (1983) 2830.
[10] R.G. Schoenberger, C.T. Chang, M. Belhoul, D.R. Torgeson, R.G. Barnes and B.J. Beaudry, *J. Less-Comm. Metals, 172–174* (1991) 411.
[11] T.T. Phua, B.J. Beaudry, D.T. Peterson, D.R. Torgeson, R.G. Barnes, M. Belhoul, G.A. Styles and E.F.W. Seymour, *Phys. Rev. B, 28* (1983) 6227.
[12] W.C. Harper and R.G. Barnes, *J. Magn. Res., 21* (1976) 507.
[13] N. Bloembergen, E.M. Purcell and R.V. Pound, *Phys. Rev., 73* (1948) 679.
[14] P. Fischer, W. Hälg, L. Schlapbach and K. Yvon, *J. Less-Comm. Metals, 60* (1978) 1.